Global and local impacts of delayed mercury mitigation efforts

Hélène Angot[1,*], *Nicholas Hoffman*[2], *Amanda Giang*[1,3], *Colin P. Thackray*[4], *Ashley N. Hendricks*[5], *Noel R. Urban*[5], *Noelle E. Selin*[1,2]

[1]Institute for Data, Systems, and Society, Massachusetts Institute of Technology, Cambridge, MA 02139, USA.

[2]Department of Earth, Atmospheric, and Planetary Sciences, Massachusetts Institute of Technology, Cambridge, MA 02139, USA.

[3]Institute for Resources, Environment and Sustainability, University of British Columbia, Vancouver, BC Canada V6T 1Z4.

[4]Harvard John A. Paulson School of Engineering and Applied Sciences, Harvard University, Cambridge, MA 02138, USA.

[5]Civil and Environmental Engineering Department, Michigan Technological University, Houghton, MI 49931, USA.

[*]angot@mit.edu

SUPPORTING INFORMATION

Table of contents

1. Methods

1.1 Local-scale impacts and Legacy penalty

We performed tests based on simulations listed in Table 1 to check the robustness of our method (described in Section 2.1).

a) We checked the consistency of year 2010 Hg global deposition with the global biogeochemical cycle (GBC) model and the chemical transport model (CTM). Global Hg deposition was 5974.8 Mg with the GBC vs. 5943.7 Mg with the CTM (BASE simulations). Given the use of different emissions inventories (see Section 2.2), this difference of 31.1 Mg (< 1%) was assumed to be negligible.

b) We then assessed whether the contribution to global deposition of year 2010 primary anthropogenic emissions, given by the difference in deposition between BASE and PRE-2010 LEGACY simulations (see Table 1), was similar. With the GBC model, assuming that primary anthropogenic emissions were completely eliminated as of 2010 led to a global Hg deposition of 4344.7 Mg. Year 2010 anthropogenic emissions therefore contributed 27.3% of total Hg deposition. A similar assumption with the CTM led to a global Hg deposition of 4110.7 Mg and a contribution to deposition of year 2010 anthropogenic emissions of 30.8%. These results are in very good agreement with those reported by Amos et al.[1], who showed that primary anthropogenic emissions account for ca. 27 % of present-day atmospheric deposition.

c) Finally, we compared FUTURE simulations. With the GBC model, we assumed a Current Policy (CP) scenario[2] from 2009 onward (*i.e.*, a 3.02 Mg yr^{-1} increase of primary anthropogenic emissions). Similarly, the CTM was run with the 2035 CP gridded emissions inventory developed by Pacyna et al.[2]. We expect global Hg deposition values to be different since emissions during the 2010-2035 period are not taken into account in the CTM. Additionally, the difference is

expected to be equal to the global legacy penalty, *i.e.,* the contribution to year 2035 deposition of 2010-2035 global emissions. We calculated a global legacy penalty (given by the difference in deposition between PRE-2035 and PRE-2010 LEGACY simulations using the GBC model) of 615 Mg (see Table 2). FUTURE simulations with the GBC model and the CTM respectively gave global Hg deposition of 6652.3 Mg and 6011.9 Mg for year 2035, *i.e.*, a difference of 640.4 Mg. Given the 31.1 Mg difference reported in S.I. Section 1.1.a, the effective difference between future GBC and CTM simulations was 609 Mg, *i.e.,* within 1% of the global legacy penalty.

1.2 Fish contamination

a) Model parameterization

Hg species represented in the lake model are Hg(0), Hg(II), and MeHg. Modeled physico-chemical processes include redox reactions (Hg(0)↔Hg(II)), methylation (Hg(II)→MeHg), demethylation (MeHg→Hg(II)), photo-demethylation (MeHg→Hg(0)), thermocline dispersion, partitioning, diffusion in sediments, settling, burial, and resuspension[3,4]. Hg(II) and Hg(p) dry deposition to the lake surface were assumed to be 10% of deposition to the catchment due to different roughness and friction velocities[3–5]. Hg(0) dry deposition to lake surface was calculated using equations developed by Hendricks[3] and based on principles of mass transfer at the air-water interface. Since GEOS-Chem does not provide deposition fluxes for MeHg, we estimated MeHg dry and wet deposition by multiplying a deposition velocity[4] by an atmospheric MeHg concentration of 2.00×10^{-12} mg L^{-1}, typical for remote regions[4,6]. The Hg runoff coefficient was set at 0.20[3,4,6], and we used resuspension and burial velocities of 1.01×10^{-5} and 2.74×10^{-6} m day^{-1}, respectively[6]. The model is based on the characteristics of the lake(s) of interest (*e.g.,* depth, retention time) and its watershed (*e.g.,* surface area). A summary of some characteristics of the 20 lakes within the

study area (see Fig.S2) is presented in Table S1: all these data are from a study initiated by the Maine Department of Environmental Protection in 1993[7], except the percentage of wetland.

To calculate the percentage of wetland in the catchment of each lake studied, data from the National Wetlands Inventory (NWI, https://www.fws.gov/wetlands/) were superimposed on data from the Watershed Boundary Dataset (WBD, https://nhd.usgs.gov/wbd.html) and the National Hydrography Dataset (NHD, https://nhd.usgs.gov) in ArcGIS. The NWI is a dataset developed by the U.S. Fish and Wildlife Service that currently exists in its second implementation at a resolution of 1:24000. It is a spatial representation of all the wetlands in the U.S. The WBD is produced by the Subcommittee on Spatial Water Data, an intergovernmental data department, and it offers hierarchically nested delineations of watershed boundaries across the U.S. This study made use of "subwatershed" or HU12 data, the most precisely delineated watershed boundaries currently available. The NHD results from a joint effort of EPA and USGS, and among its products is a spatial catalogue of all lakes and ponds in the U.S. Comparing the WBD and NHD, we located the particular subwatersheds that encompassed every lake of interest. In the one case where a lake crossed the border between two subwatersheds, those two subwatersheds were merged and treated as a single watershed. Inspection of the intersection of each sub-watershed of interest with the land use data from the NWI allowed for the calculation within each sub-watershed of the percentage of wetland by area. To calculate this percentage, we divided the area in each catchment classified as wetland by the total catchment area. Results are presented in Table S1.

To estimate values not directly reported by the Maine Department of Environmental Protection[7] but needed as inputs in the model, we multiplied known values by ratios of values from Hendricks[3]. Table S2 lists the relevant parameters from Hendricks[3] and whether or not they exist in the 1993 study[7]. Table S3 lists all of the ratios used based on the values in Table S2. We multiplied known

values for our 20 lakes by these ratios to estimate unknown values. For example, to estimate the thermocline area of a given lake, we multiplied the ratio of thermocline area over lake surface area from Hendricks[3] by the lake surface area reported in the 1993 study[7].

The model is also driven by Hg deposition fluxes from GEOS-Chem. Results from the present-day (2009-2015) BASE simulation performed with GEOS-Chem (see Table 1) were evaluated against available observations. The mean (± standard deviation) modeled Hg(0) atmospheric concentration in Maine tribal areas is 1.34 ± 0.03 ng m^{-3}. Although slightly lower than the Northern Hemisphere atmospheric background of ~1.50 ng m^{-3} reported by Sprovieri et al.[8], this result compares well with the 2009-2015 mean Hg(0) concentration of 1.32 ± 0.23 ng m^{-3} at Kejimkujik National Park, Nova Scotia (Canada). This rural site is located ~400 km further south-east and is part of the US/Canadian Atmospheric Mercury Network[9] (AMNet, http://nadp.slh.wisc.edu/AMNet/). The 2009-2015 mean modeled wet deposition flux is 5.2 ± 0.23 μg m^{-2} yr^{-1}, compared with a mean measured flux of 6.4 ± 1.1 μg m^{-2} yr^{-1} reported at Caribou (Maine, USA) as part of the Mercury Deposition Network[10] (http://nadp.slh.wisc.edu/mdn/). This site is located ~20 km north of Presque Isle (see Fig.S2). Finally, the mean modeled dry deposition is 13.2 ± 0.4 μg m^{-2} yr^{-1}, while the estimated flux is ~15 μg m^{-2} yr^{-1} at Presque Isle[11].

b) Model calibration

The model as implemented by Perlinger et al.[4] was calibrated for a lake in Michigan's Upper Peninsula. To better calibrate the model for lakes in Maine, we performed a factorial experiment on the methylation and demethylation rates. We sampled five points evenly spaced within a distribution of values found in the literature and ran the model for every possible combination of the five points over the two parameters, which is equivalent to 5^2 combinations. Then a least squares regression was performed in order to find the set of parameters which yielded the minimum

distance between the modeled and measured MeHg values across two different (but overlapping) randomly selected sets of ten (out of twenty) lakes. The square of the difference between the measured whole (rather than fillet[12]) piscivore MeHg concentrations and the modeled median piscivore MeHg concentrations from each combination of parameters used in the factorial experiment were summed over the ten lakes. The smallest sum among these 5^2 sums was chosen as representing the optimal set of parameters (methylation and demethylation rates) and implemented in the model. We used a demethylation rate of 1 day^{-1} similarly to Perlinger et al.[4], and a methylation rate of 0.20 day^{-1}, within the range of values found in the literature[3,6].

c) Model evaluation

The model was evaluated against data collected in 1993 by the Maine Department of Environmental Protection[7]. To our knowledge, there is no comparably comprehensive survey performed more recently in Maine tribal areas. For consistency with measured fish Hg concentrations, we used year 1993 Hg deposition values[13] for model evaluation. Fig.S1 shows the total Hg concentration in predatory (PF) and mixed feeders' fishes (MF) within the study area (20 lakes). While the model tends to underestimate concentrations in MF, the difference between modeled and observed median concentrations in PF (main species of interest here) is < 1 %. Additionally, summertime Hg and MeHg concentrations in the epilimnion and hypolimnion fall within the range of values measured in nearby lakes[14,15].

Table S1: Summary of some characteristics of the modeled lakes.

Lake	Surface area (m^2)	Mean depth (m)	Drainage area (m^2)	Volume (m^3)	Runoff factor	Flushing rate	Outflow rate (m^3/day)	Retention time (day)	Wetland (%)	Sediment Hg concentration (ppm)	Hg concentration in PW (ppm)*	Hg concentration in OW (ppm)*
Brackett	$2.29x10^6$	4.6	$1.90x10^7$	$9.51x10^6$	0.56	1.1	$2.9x10^4$	332	5.3	0.002	0.41 (n = 10)	0.04 (n = 10)
Bradbury	$1.60x10^5$	6.1	$4.30x10^7$	$8.90x10^5$	0.51	24.5	$6.0x10^4$	15	9.7	0.21	0.34 (n = 1)	0.24 (n = 5)
Chandler	$1.68x10^6$	4.3	$1.20x10^7$	$5.74x10^6$	0.52	1.1	$1.7x10^4$	332	10.9	0.12	0.23 (n = 3)	0.35 (n = 5)
Chase	$4.00x10^4$	5.5	$1.10x10^7$	$2.03x10^5$	0.54	28.6	$1.6x10^4$	13	3.7	0.20	0.13 (n = 2)	0.07 (n = 5)
Cross	$1.03x10^7$	6.1	$4.25x10^8$	$6.45x10^7$	0.50	3.3	$5.8x10^5$	111	30.3	0.12	0.47 (n = 5)	0.21 (n = 5)
Eagle	$2.26x10^7$	13.4	$1.97x10^9$	$3.08x10^8$	0.50	3.2	$2.7x10^6$	114	11.2	0.09	0.27 (n = 5)	0.30 (n = 5)
Grand	$5.83x10^7$	11.3	$5.85x10^8$	$6.86x10^8$	0.56	0.5	$9.4x10^5$	730	5.8	0.20	0.47 (n = 2)	0.23 (n = 4)
Keene	$3.60x10^5$	4.9	$4.00x10^6$	$6.50x10^5$	0.61	1.3	$2.3x10^3$	281	10.0	0.21	0.38 (n = 2)	0.07 (n = 5)
Lambert	$2.18x10^6$	6.1	$1.70x10^7$	$1.43x10^7$	0.58	0.7	$2.7x10^4$	521	16.5	0.31	0.39 (n = 5)	0.28 (n = 5)
Machias	$6.20x10^6$	4.0	$1.72x10^8$	$2.06x10^7$	0.56	4.7	$2.6x10^5$	78	17.9	0.12	1.2 (n = 5)	0.75 (n = 5)
Meddybemps	$2.72x10^7$	4.3	$1.16x10^8$	$1.18x10^8$	0.62	0.6	$1.9x10^5$	608	19.3	0.18	0.21 (n = 5)	-
Molunkus	$4.36x10^6$	4.6	$9.10x10^7$	$1.85x10^7$	0.52	2.5	$1.3x10^5$	146	13.7	0.22	0.70 (n = 5)	0.21 (n =5)
Monson	$3.70x10^5$	2.4	$3.80x10^7$	$7.30x10^5$	0.51	26.3	$5.3x10^4$	14	16.0	0.13	0.34 (n = 1)	0.28 (n = 1)
Orange	$9.30x10^5$	3.7	$5.00x10^7$	$2.63x10^6$	0.66	12.6	$9.1x10^4$	29	19.2	0.22	0.52 (n = 5)	0.22 (n = 5)
Pennington	$2.10x10^5$	0.9	$4.00x10^6$	$1.07x10^5$	0.51	17.5	$5.1x10^3$	21	18.4	0.09	0.16 (n = 2)	-
Pleasant	$1.40x10^6$	5.2	$8.00x10^6$	$7.35x10^6$	0.62	0.7	$1.4x10^4$	521	19.3	0.11	0.42 (n = 5)	0.13 (n = 5)
Portland	$1.66x10^5$	5.2	$4.30x10^7$	$8.60x10^5$	0.51	25.5	$6.0x10^4$	14	25.8	0.20	0.45 (n = 5)	0.06 (n = 5)
Sly Brook	$7.00x10^4$	2.7	$7.00x10^6$	$1.38x10^5$	0.50	25.2	$9.5x10^3$	14	7.7	0.17	0.94 (n = 5)	0.11 (n = 5)
Togue	$1.30x10^6$	13.1	$9.00x10^6$	$1.56x10^7$	0.56	0.3	$1.3x10^4$	1217	4.1	0.19	0.39 (n = 5)	0.17 (n = 5)
Umcolcus	$2.90x10^6$	3.0	$3.80x10^7$	$8.12x10^6$	0.61	2.9	$6.5x10^4$	126	20.9	Rocky bottom	0.51 (n = 5)	0.15 (n = 5)

*PW and OW refer to predatory and omnivore (mixed-feeder) whole fish, respectively. In parenthesis, n is the number of fish in the composite sample analyzed[7].

Table S2: Lake Geometry values from a lake in Michigan's Upper Peninsula (UP).

Parameter	Lake in Michigan's UP[3]	Available value in Maine[7]?	Calculation
Lake surface area	9 730 000 m^2	Yes	
Thermocline area	8 360 000 m^2	No	$\left[\frac{\text{thermocline area}}{\text{lake surf. area}}\right]_{Michigan} \times [lake\ surf.\ area]_{Maine}$
Sediment area	8 360 000 m^2	No	$\left[\frac{\text{sediment area}}{\text{lake surf. area}}\right]_{Michigan} \times [\text{lake surf. area}]_{Maine}$
Total volume	142 483 600 m^3	Yes	
Epilimnion volume	84 600 000 m^3	No	$\left[\frac{\text{epilimnion volume}}{\text{total volume}}\right]_{Michigan} \times [total\ volume]_{Maine}$
Hypolimnion volume	57 800 000 m^3	No	$\left[\frac{\text{hypolimnion volume}}{\text{total volume}}\right]_{Michigan} \times [total\ volume]_{Maine}$
Sediment volume	83 600 m^3	No	$\left[\frac{\text{sediment volume}}{\text{total volume}}\right]_{Michigan} \times [total\ volume]_{Maine}$

Table S3: Ratios of lake characteristics from a lake in Michigan's Upper Peninsula (UP).

Ratio	Lake in Michigan's UP[3]
Thermocline area/lake surface area	0.859
Epilimnion volume/total volume	0.594
Hypolimnion volume/total volume	0.406
Sediment volume/total volume	0.00059

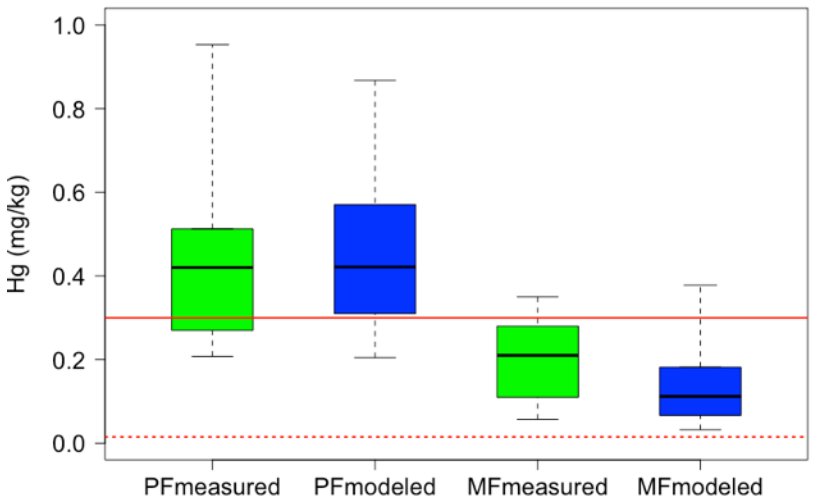

Figure S1: Lake Hg model evaluation. Total Hg concentration (mg kg^{-1}) in predatory (PF) and mixed feeders' fishes (MF) within the study area (20 lakes). Measured and modeled values are in green and blue, respectively. The straight red line represents the 0.3 mg kg^{-1} US EPA threshold[16] and the dotted red line a safe level target of 0.018 mg kg^{-1} for a desired subsistence fish consumption of 300-500 grams per day[4,17,18]. Boxes, inside lines, and whiskers indicate interquartile range, median, 5th and 95th percentiles, respectively.

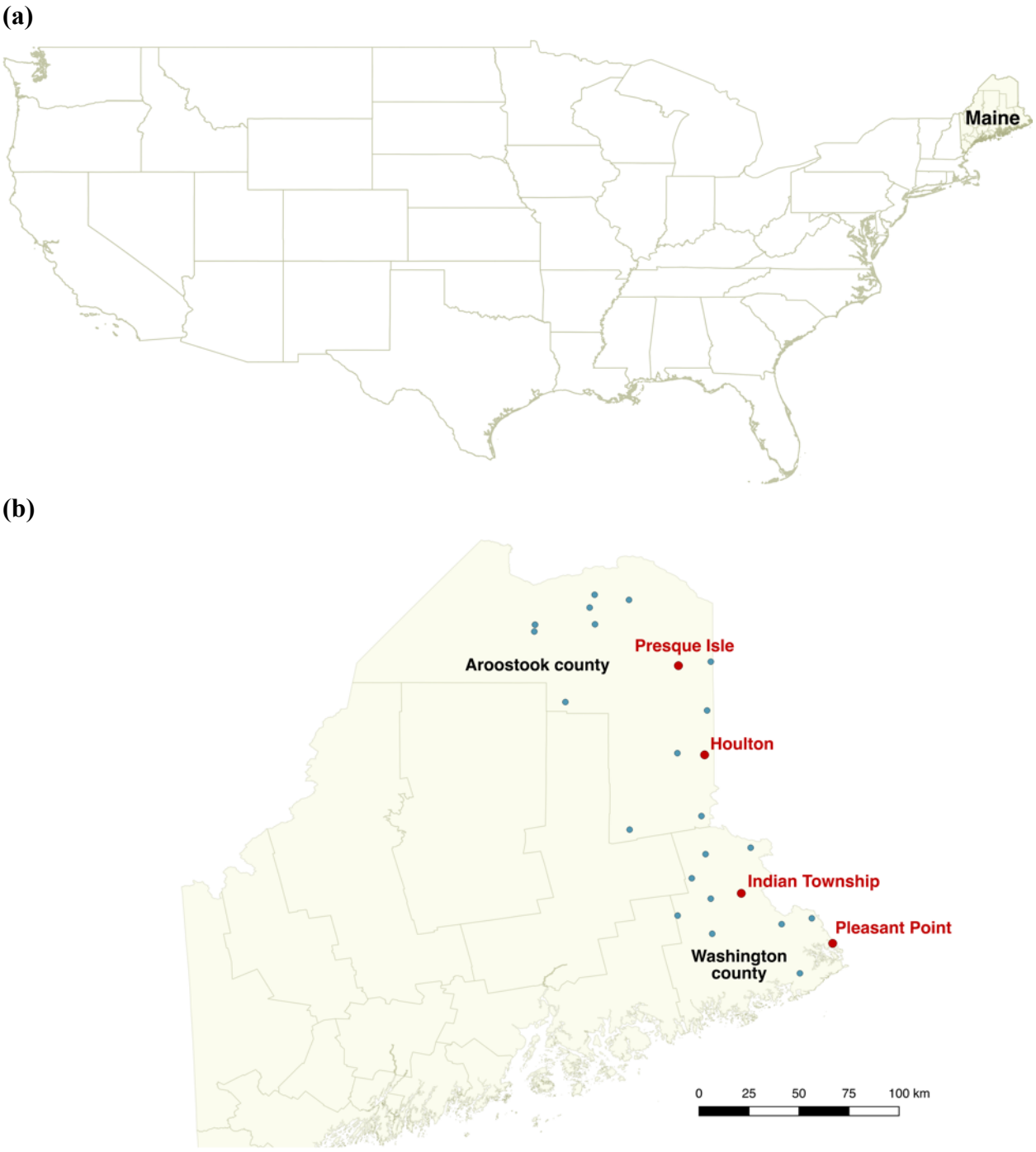

Figure S2: (a) Location of Maine, the easternmost state in the contiguous United States of America. **(b)** The Aroostook Band of Micmacs is based in Presque Isle, the Houlton Band of Maliseets in Houlton, and the Passamaquoddy Tribe in both Indian Township and Pleasant Point. Together with the Penobscot Nation established further south-west, they represent approximately 8000 Native people in Maine, known collectively as the Wabanaki ("People of the Dawn"). Blue dots: lakes of interest. This Figure was made using QGIS (version 2.18).

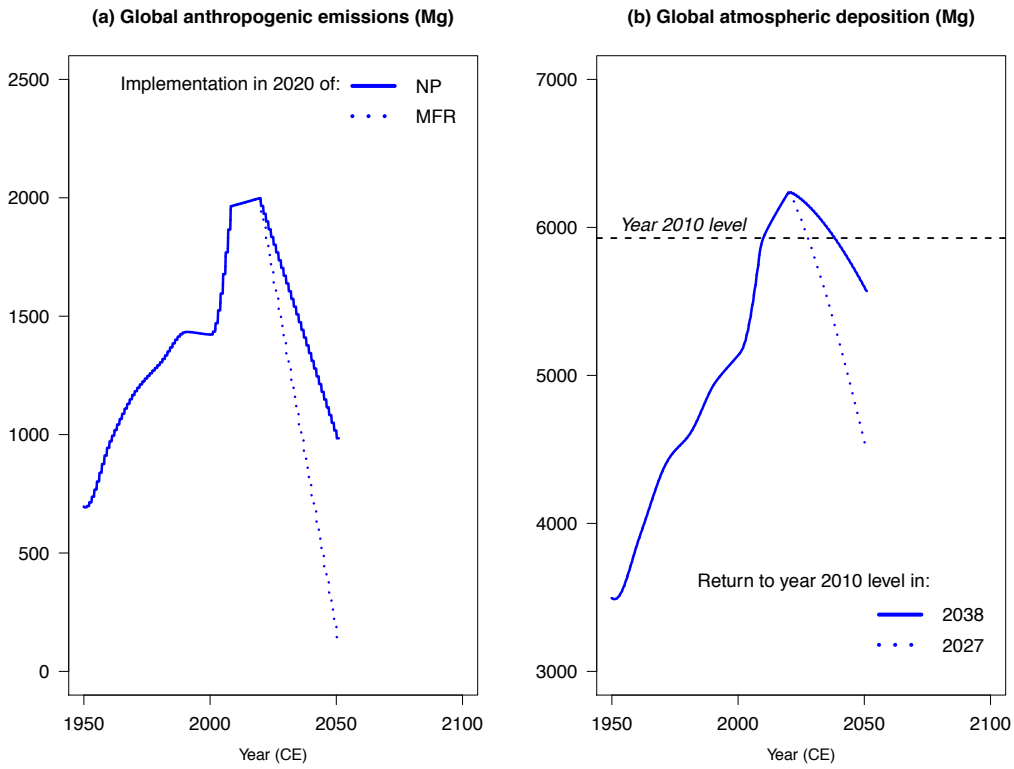

Figure S3: (a) Global primary anthropogenic emissions of Hg to the atmosphere (in Mg). New Policy (NP, solid line) and Maximum Feasible Reduction (MFR, dotted line) scenarios are implemented in 2020. (b) Global atmospheric Hg deposition to ecosystems (in Mg). Return of Hg deposition to its year 2010 level (chosen for illustrative purposes) is achieved in 2038 or 2027 in case of NP (solid line) or MFR (dotted line) implementation, respectively.

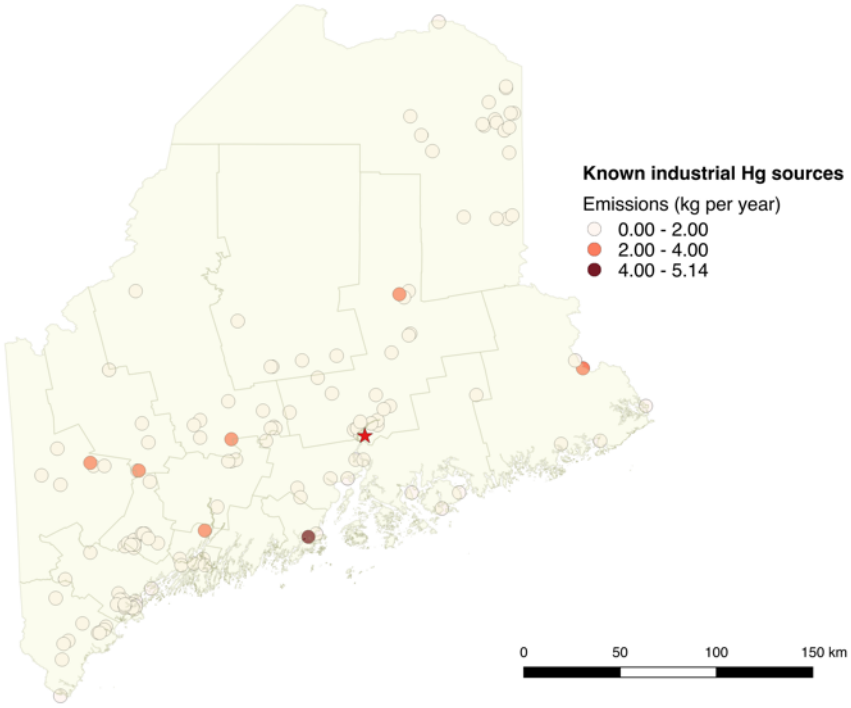

Figure S4: Hg emissions (kg yr^{-1}) from known industrial sources in Maine according to the 2011 National Emissions Inventory (NEI) prepared by the United States Environmental Protection Agency (U.S. EPA)[19]. Annual emissions in Maine are at the low end of state-level emissions in the United States (see Fig.S4). The red star shows the location of extensive Hg releases to the Penobscot River (1967-2000) by a chlor-alkali production facility, HoltraChem[20–23]. Due to the presence of a known industrial contamination, lakes in Penobscot Nation tribal lands were excluded from this study. This Figure was made using QGIS (version 2.18).

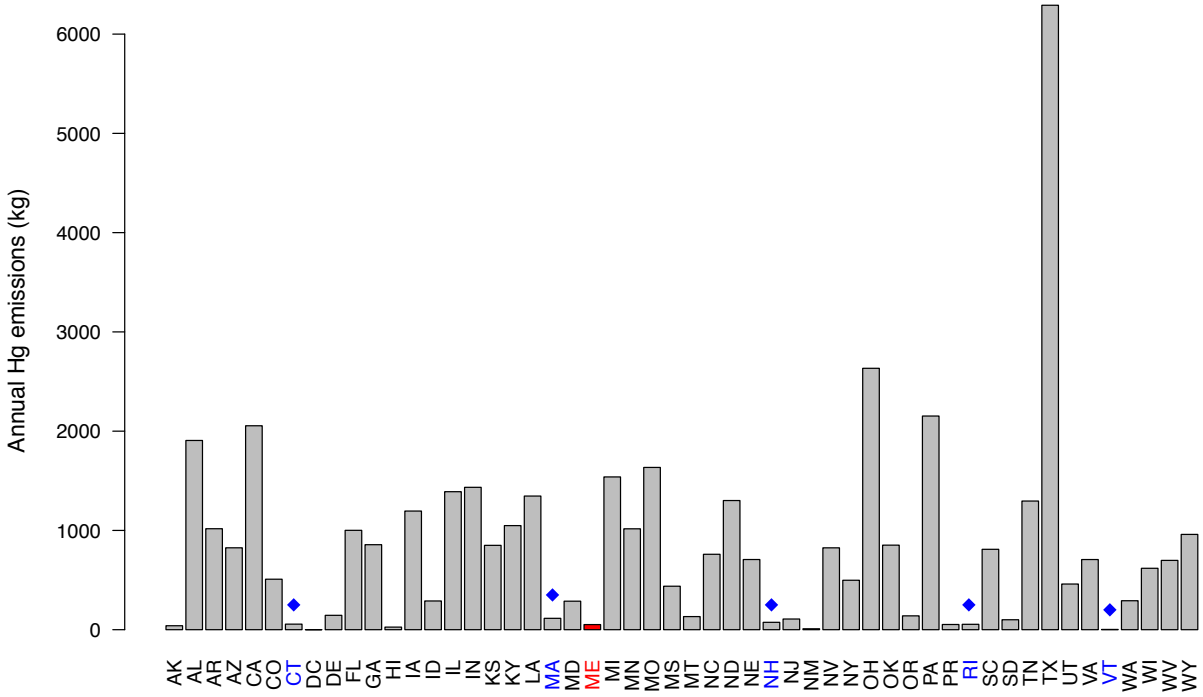

Figure S5: Year 2011 U.S. state-level Hg emissions (kg) by known industrial sources according to the 2011 National Emissions Inventory (NEI) prepared by the United States Environmental Protection Agency (U.S. EPA)[19]. Emissions in Maine (ME, in red) and neighboring New England states (CT, MA, NH, RI, VT, blue diamonds) are at the low end of state-level emissions in the United States. AK: Alaska, AL: Alabama, AR: Arkansas, AZ: Arizona, CA: California, CO: Colorado, CT: Connecticut, DC: District of Columbia, DE: Delaware, FL: Florida, GA: Georgia, HI: Hawaii, IA: Iowa, ID: Idaho, IL: Illinois, IN: Indiana, KS: Kansas, KY: Kentucky, LA: Louisiana, MA: Massachusetts, MD: Maryland, ME: Maine, MI: Michigan, MN: Minnesota, MO: Missouri, MS: Mississippi, MT: Montana, NC: North Carolina, ND: North Dakota, NE: Nebraska, NH: New Hampshire, NJ: New Jersey, NM: New Mexico, NV: Nevada, NY: New York, OH: Ohio, OK: Oklahoma, OR: Oregon, PA: Pennsylvania, PR: Puerto Rico, RI: Rhode Island, SC: South Carolina, SD: South Dakota, TN: Tennessee, TX: Texas, UT: Utah, VA: Virginia, VT: Vermont, WA: Washington, WI: Wisconsin, WV: West Virginia, WY: Wyoming.

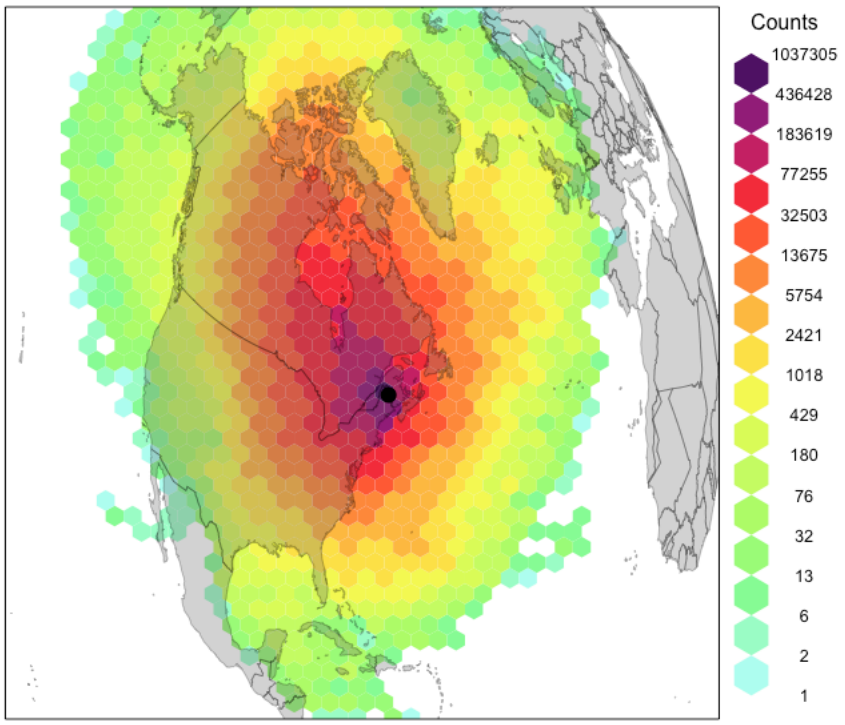

Figure S6: Origin of air masses influencing Maine tribal areas. Gridded back trajectory frequencies using an orthogonal map projection, with hexagonal binning. The tiles represent the number of incidences. 2007-2016 hourly back trajectories were computed using the HYSPLIT model[24] and the figure was made using the R package openair[25]. Maine tribal areas are mainly influenced by air masses originating from Canada and the Arctic (Hudson Bay), *i.e.*, the Northern Hemisphere atmospheric background, rather than U.S. emissions. The black dot shows the location of Presque Isle (ME, USA).

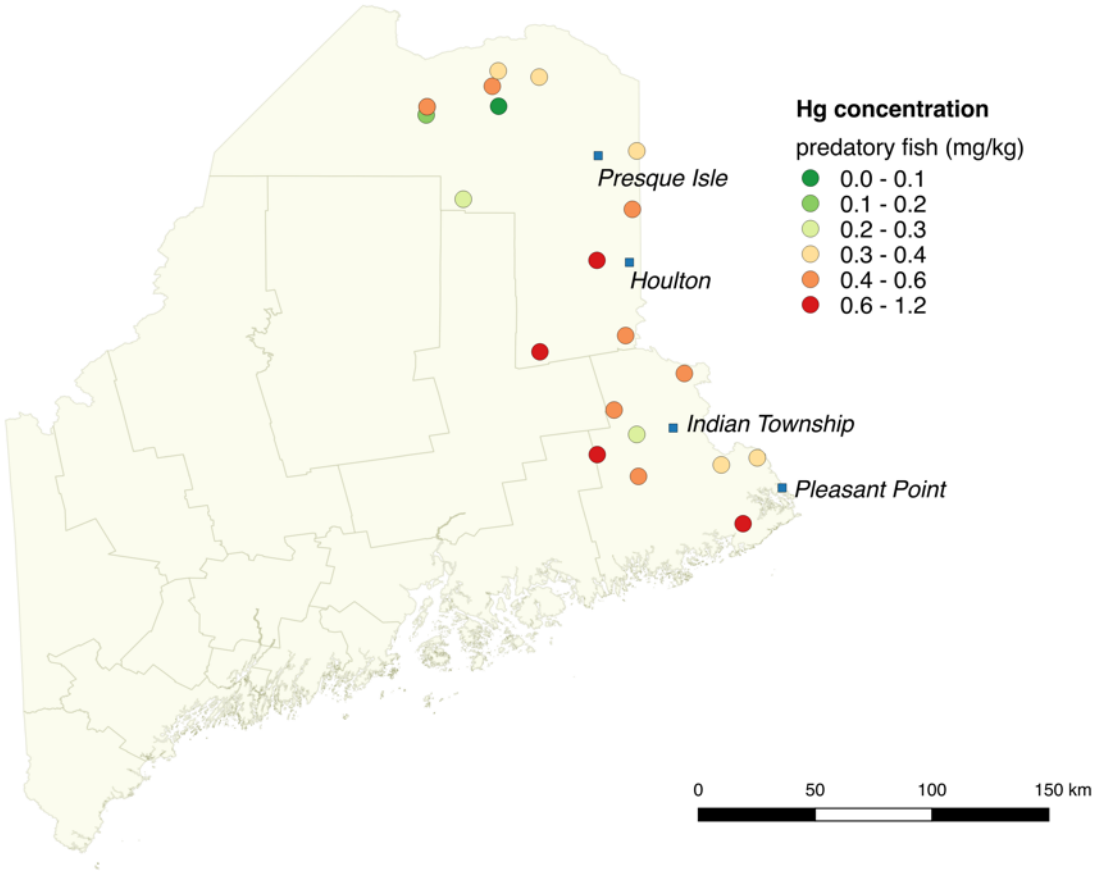

Figure S7: Total Hg concentration (mg kg^{-1}) in predatory fish fillets collected in lakes within the study area. Data are from a study initiated by the Maine Department of Environmental Protection in 1993[7]. 16 out of 20 lakes presented concentrations above the 0.3 mg kg^{-1} US EPA threshold[16]. This Figure was made using QGIS (version 2.18).

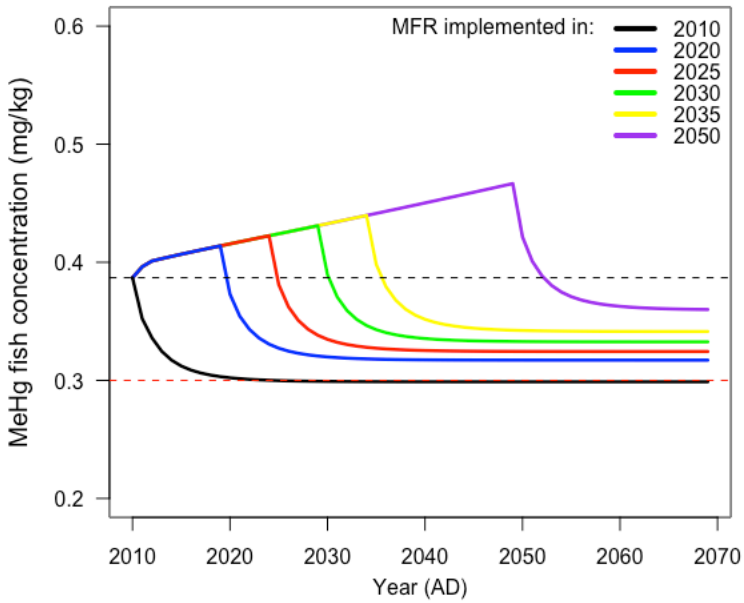

Figure S8: Median response of Eastern Maine (USA) lacustrine predatory fish contamination to delayed implementation of a Maximum Feasible Reduction (MFR) scenario. Black dashed line: year 2010 MeHg concentration. Red dashed line: U.S. EPA reference dose for MeHg (0.3 mg kg^{-1}).

References

(1) Amos, H. M.; Jacob, D. J.; Streets, D. G.; Sunderland, E. M. Legacy Impacts of All-Time Anthropogenic Emissions on the Global Mercury Cycle. *Global Biogeochem. Cycles* **2013**, *27* (2), 410–421.

(2) Pacyna, J. M.; Travnikov, O.; De Simone, F.; Hedgecock, I. M.; Sundseth, K.; Pacyna, E. G.; Steenhuisen, F.; Pirrone, N.; Munthe, J.; Kindbom, K. Current and Future Levels of Mercury Atmospheric Pollution on a Global Scale. *Atmos. Chem. Phys.* **2016**, *16* (19), 12495–12511.

(3) Hendricks, A.N. A Model to Predict Concentrations and Uncertainty for Mercury Species in Lakes. Open Access Master's Thesis, Michigan Technological University: http://digitalcommons.mtu.edu/etdr/585, 2018.

(4) Perlinger, J. A.; R. Urban, N.; Giang, A.; E. Selin, N.; N. Hendricks, A.; Zhang, H.; Kumar, A.; Wu, S.; S. Gagnon, V.; S. Gorman, H.; et al. Responses of Deposition and Bioaccumulation in the Great Lakes Region to Policy and Other Large-Scale Drivers of Mercury Emissions. *Environmental Science: Processes & Impacts* **2018**, *20* (1), 195–209.

(5) Kwan, J.; Taylor, P. A. On Gas Fluxes from Small Lakes and Ponds. *Boundary-Layer Meteorol* **1994**, *68* (4), 339–356.

(6) Knightes, C. D. Development and Test Application of a Screening-Level Mercury Fate Model and Tool for Evaluating Wildlife Exposure Risk for Surface Waters with Mercury-Contaminated Sediments (SERAFM). *Environmental Modelling & Software* **2008**, *23* (4), 495–510.

(7) US EPA. Region 1 Fish Tissue Contamination QA Plan | Regional Environmental Monitoring and Assessment Program | US EPA https://archive.epa.gov/emap/archive-emap/web/html/reg1_rpt.html (accessed May 8, 2018).

(8) Sprovieri, F.; Pirrone, N.; Bencardino, M.; D'Amore, F.; Carbone, F.; Cinnirella, S.; Mannarino, V.; Landis, M.; Ebinghaus, R.; Weigelt, A.; et al. Atmospheric Mercury Concentrations Observed at Ground-Based Monitoring Sites Globally Distributed in the Framework of the GMOS Network. *Atmos. Chem. Phys.* **2016**, *16* (18), 11915–11935.

(9) Gay, D. A.; Schmeltz, D.; Prestbo, E.; Olson, M.; Sharac, T.; Tordon, R. The Atmospheric Mercury Network: Measurement and Initial Examination of an Ongoing Atmospheric Mercury Record across North America. *Atmos. Chem. Phys.* **2013**, *13* (22), 11339–11349.

(10) Prestbo, E. M.; Gay, D. A. Wet Deposition of Mercury in the U.S. and Canada, 1996–2005: Results and Analysis of the NADP Mercury Deposition Network (MDN). *Atmospheric Environment* **2009**, *43* (27), 4223–4233.

(11) Zhang, L.; Wu, Z.; Cheng, I.; Wright, L. P.; Olson, M. L.; Gay, D. A.; Risch, M. R.; Brooks, S.; Castro, M. S.; Conley, G. D.; et al. The Estimated Six-Year Mercury Dry Deposition Across North America. *Environ. Sci. Technol.* **2016**, *50* (23), 12864–12873.

(12) Hammerschmidt, C. R.; Fitzgerald, W. F. Bioaccumulation and Trophic Transfer of Methylmercury in Long Island Sound. *Arch Environ Contam Toxicol* **2006**, *51* (3), 416–424.

(13) Muntean, M.; Janssens-Maenhout, G.; Song, S.; Selin, N. E.; Olivier, J. G. J.; Guizzardi, D.; Maas, R.; Dentener, F. Trend Analysis from 1970 to 2008 and Model Evaluation of EDGARv4 Global Gridded Anthropogenic Mercury Emissions. *Science of The Total Environment* **2014**, *494–495*, 337–350.

(14) Dennis, I. F.; Clair, T. A.; Driscoll, C. T.; Kamman, N.; Chalmers, A.; Shanley, J.; Norton, S. A.; Kahl, S. Distribution Patterns of Mercury in Lakes and Rivers of Northeastern North America. *Ecotoxicology* **2005**, *14* (1–2), 113–123.
(15) Driscoll, C. T.; Han, Y.-J.; Chen, C. Y.; Evers, D. C.; Lambert, K. F.; Holsen, T. M.; Kamman, N. C.; Munson, R. K. Mercury Contamination in Forest and Freshwater Ecosystems in the Northeastern United States. *BioScience* **2007**, *57* (1), 17–28.
(16) US EPA. Water Quality Criteria: Notice of Availability of Water Quality Criterion for the Protection of Human Health: Methylmercury https://www.federalregister.gov/documents/2001/01/08/01-217/water-quality-criteria-notice-of-availability-of-water-quality-criterion-for-the-protection-of-human (accessed May 8, 2018).
(17) Gagnon, V.; Gorman, H.; Norman, E. Power and Politics in Research Design and Practice: Opening up Space for Social Equity in Interdisciplinary, Multi-Jurisdictional and Community-Based Research. *Gateways: International Journal of Community Research and Engagement* **2017**, *10* (0), 164–184.
(18) US EPA. Wabanaki Traditional Cultural Lifeways Exposure Scenario https://www.epa.gov/tribal/wabanaki-traditional-cultural-lifeways-exposure-scenario (accessed May 8, 2018).
(19) US EPA. 2011 National Emissions Inventory (NEI) Data https://www.epa.gov/air-emissions-inventories/2011-national-emissions-inventory-nei-data (accessed May 8, 2018).
(20) Santschi, P. H.; Yeager, K. M.; Schwehr, K. A.; Schindler, K. J. Estimates of Recovery of the Penobscot River and Estuarine System from Mercury Contamination in the 1960's. *Science of The Total Environment* **2017**, *596–597*, 351–359.
(21) Yeager, K. M.; Schwehr, K. A.; Louchouarn, P.; Feagin, R. A.; Schindler, K. J.; Santschi, P. H. Mercury Inputs and Redistribution in the Penobscot River and Estuary, Maine. *Sci Total Environ* **2017**, *622–623*, 172–183.
(22) Sunderland, E. M.; Amirbahman, A.; Burgess, N. M.; Dalziel, J.; Harding, G.; Jones, S. H.; Kamai, E.; Karagas, M. R.; Shi, X.; Chen, C. Y. Mercury Sources and Fate in the Gulf of Maine. *Environ Res* **2012**, *119*, 27–41.
(23) Evers, D. C.; Han, Y.-J.; Driscoll, C. T.; Kamman, N. C.; Goodale, M. W.; Lambert, K. F.; Holsen, T. M.; Chen, C. Y.; Clair, T. A.; Butler, T. Biological Mercury Hotspots in the Northeastern United States and Southeastern Canada. *BioScience* **2007**, *57* (1), 29–43.
(24) Stein, A. F.; Draxler, R. R.; Rolph, G. D.; Stunder, B. J. B.; Cohen, M. D.; Ngan, F. NOAA's HYSPLIT Atmospheric Transport and Dispersion Modeling System. *Bull. Amer. Meteor. Soc.* **2015**, *96* (12), 2059–2077.
(25) Carslaw, D.; Ropkins, K. Openair - An R Package for Air Quality Data Analysis. *Environ Modell Softw* **2012**, *27–28*, 52–61.